Surface resonances at transition metal dichalcogenide heterostructures

C. Kreis, S. Werth, R. Adelung, L. Kipp, and M. Skibowski
Institut für Experimentelle und Angewandte Physik, Universität Kiel, D-24118 Kiel, Germany

D. Voß, P. Krüger, A. Mazur, and J. Pollmann
Institut für Festkörpertheorie, Universität Münster, D-48149 Münster, Germany
(Received 27 November 2001; published 4 April 2002)

Layered transition metal dichalcogenides do generally not exhibit characteristic electronic surface states localized perpendicular to the layers. Employing van der Waals epitaxy together with angle-resolved photoemission spectroscopy we show how surface-layer-derived electronic states can be generated on these materials. For a heterojunction consisting of one HfS_2 epilayer adsorbed on bulk WSe_2, purely two-dimensional behavior as well as three-dimensional coupling of the epilayer to substrate bulk states is observed despite a large lattice mismatch between epilayer and substrate. The experimental results are discussed in the context of electronic structure calculations.

DOI: 10.1103/PhysRevB.65.153314 PACS number(s): 73.21.−b, 71.20.Nr, 79.60.Jv

The broken translational symmetry at surfaces of crystalline materials, in general, can lead to localized surface states and surface resonances. These features are two-dimensionally periodic parallel to the surface. If the energy of these states lies within a band gap of the projected band structure of the bulk material, they are exponentially localized perpendicular to the surface. Surface resonances overlap in energy with bulk bands and usually extend several layers into the bulk because they can mix with bulk states.

Two-dimensional layered materials of the transition metal dichalcogenide (TMDC) family, consisting of chalcogen-metal-chalcogen triple layers bonded by van der Waals interactions only,[1] generally do not exhibit surface derived states. This is due to the absence of broken bonds at their surface. Electronic states whose wave functions are mainly localized at the surface—which we label as surface-layer-derived states in the following—can relatively easily be generated, however, by heteroepitaxial growth of one kind of a chalcogen-metal-chalcogen triple layer on a different layered substrate material. Even in the case of a large lattice mismatch between epilayer and substrate such adlayers can be grown smoothly with their own lattice constant by van der Waals epitaxy (VDWE).[2] This way, it is possible to grow a large variety of insulating, semiconducting, or metallic TMDC heterojunctions[3,4] which are of technological importance in the field of photovoltaics[5] and in high-energy-density batteries.[6] WSe_2, e.g., is a prototype for high-efficiency solar cells.[7]

More recently, Klein *et al.*[8] have shown that surface states on InSe layers prepared by van der Waals epitaxy on graphite do not couple to substrate states and exhibit a purely two-dimensional character, therefore. In this case, the energy of the InSe surface layer states lies within a projected gap of the graphite substrate band structure so that the surface-layer-derived states do not interact with the substrate states.

On the contrary, here we are dealing with the opposite case in which the energy of all surface-layer-derived states coincides with the projected substrate bulk bands. In particular, we investigate which states exhibit merely two-dimensional character and which display in addition electronic coupling to the substrate, i.e., in the third dimension, through surface-derived states. The latter coupling across the heterointerface between two different TMDC layered materials could be the key for an understanding of the van der Waals epitaxy of these materials.

In this work we report results of angle-resolved photoelectron spectroscopy (ARPES) with synchrotron radiation showing the evolution of electronic surface resonances at the surface of a layered material. A semiconductor heterostructure consisting of a S-Hf-S triple layer—i.e., of one HfS_2 ''monolayer'' on *p*-doped WSe_2—serves as a model system for assessing the properties of surface-layer-derived states and their coupling behavior to bulk states of the substrate material. In our investigations of this system we demonstrate that the surface-layer-derived electronic states are either fully localized in the surface layer or couple to bulk states of the underlying substrate material. This coupling occurs in spite of the broken translational symmetry due to the lattice mismatch parallel to the layers. The interpretation of our experimental data is supported by the results of our band structure calculations and layer-resolved electron densities of states.

All results described here were obtained on clean HfS_2 monolayers epitaxially grown on bulk WSe_2. Growth parameters (sulphur pressure $p_{S_2} \sim 2-3\times10^{-9}$ mbar, substrate temperature $T_S = 650$ K, and a low hafnium flux) were chosen to yield a growth rate of about one HfS_2 monolayer per hour. Preparations were characterized employing low-energy electron diffraction (LEED) and *in situ* scanning tunneling microscopy (STM). Subsequently the samples were transported under ultrahigh-vacuum conditions to the Hamburg Synchrotron Radiation Laboratory. Photoemission spectra were taken at the HONORMI beamline using our angular spectrometer for photoelectrons with high-energy resolution ASPHERE (Ref. 9) (the overall energy resolution was chosen to be $\Delta E = 65$ meV).

The calculations of the band structures and charge densities of $2H_b$-WSe_2 and $1T$-HfS_2 were performed employing density functional theory (DFT) within a local-density approximation (LDA).[10] Norm-conserving, nonlocal pseudopo-

 ©2002 The American Physical Society

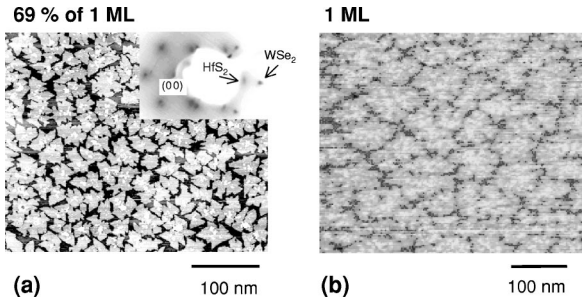

FIG. 1. STM pictures of (a) 69% of 1 ML and (b) 1 ML HfS_2/WSe_2 [(a) empty states, 2V bias, $I_t=0.5$ nA, substrate temperature $T_{sub}=600$ K (b) 1 V bias, $I_t=0.24$ nA, $T_{sub}=650$ K]. inset (a): corresponding LEED image ($E_{kin}=150$ eV).

tentials as suggested by Bachelet, Hamann, and Schlüter[11] have been used. The exchange-correlation energy was taken into account using the Ceperley-Alder[12] form as parametrized by Perdew and Zunger.[13] To represent the wave functions, Gaussian orbitals of *s*, *p*, *d*, and *s** symmetry have been employed. For WSe_2 and HfS_2 we have used 100 and 120 orbitals per unit cell and spin, respectively, which were localized at the atomic positions. The decay constants of the Gaussians were chosen to be {0.17, 0.45, 1.18, 3.10} for W, {0.17, 0.41, 1.00} for Se, {0.17, 0.45, 1.10, 2.50} for Hf, and {0.17, 0.47, 0.90, 1.70} for S (in atomic units). A linear mesh of less than 0.2 Å in real space was used for the representation of the charge density and the potential. The spin-orbit interaction was taken into account in each step of the iteration in an on-site approximation; i.e., only integrals with the same location of the Gaussian orbitals and the spin-orbit potential were taken into account. The lattice parameters used in the calculations are $a=3.280$ Å, $c=2\times6.475$ Å, and $z=0.129c$ for WSe_2, and $a=3.635$ Å, $c=5.837$ Å, and $z=0.25c$ for HfS_2, where *z* is the distance between the metal layer and the enclosing chalcogen layers.

Epitaxial growth of the first HfS_2 monolayer is characterized by STM and LEED (Fig. 1). During the initial stages of growth two-dimensional HfS_2 islands are formed [Fig. 1(a)]. The corresponding LEED picture [inset in Fig. 1(a)] consists of two hexagonal patterns with the outer one belonging to WSe_2 and the inner one to HfS_2 due to its larger lattice constant [$a_{WSe_2}=3.286$ Å, $a_{HfS_2}=3.635$ Å. (Ref. 14)]. From the relative size of both patterns a lattice mismatch of $11\%\pm1\%$ is ascertained. Thus HfS_2 grows with its own bulk lattice constant as a consequence of the weak interaction between substrate and epilayer. The alignment of both patterns shows that the HfS_2 clusters have the same crystallographic orientation as the WSe_2 substrate. The islands increase in size to form the first monolayer (1 ML) upon coalescence [Fig. 1 (b)]. Note that the second monolayer at this stage of growth has almost not started, yet, and a well-defined thickness of one monolayer HfS_2 is obtained.

Considering first the electronic structure $E(k_\perp)$ perpendicular to the surface of bulk HfS_2 we applied ARPES at normal emission with various photon energies $h\nu$ [Fig. 2(a)]. Two pronounced peaks marked *A* and *B* are observed which are associated with sulphur derived states. Emission *B* displays a large dispersion of ~800 meV while peak *A* only

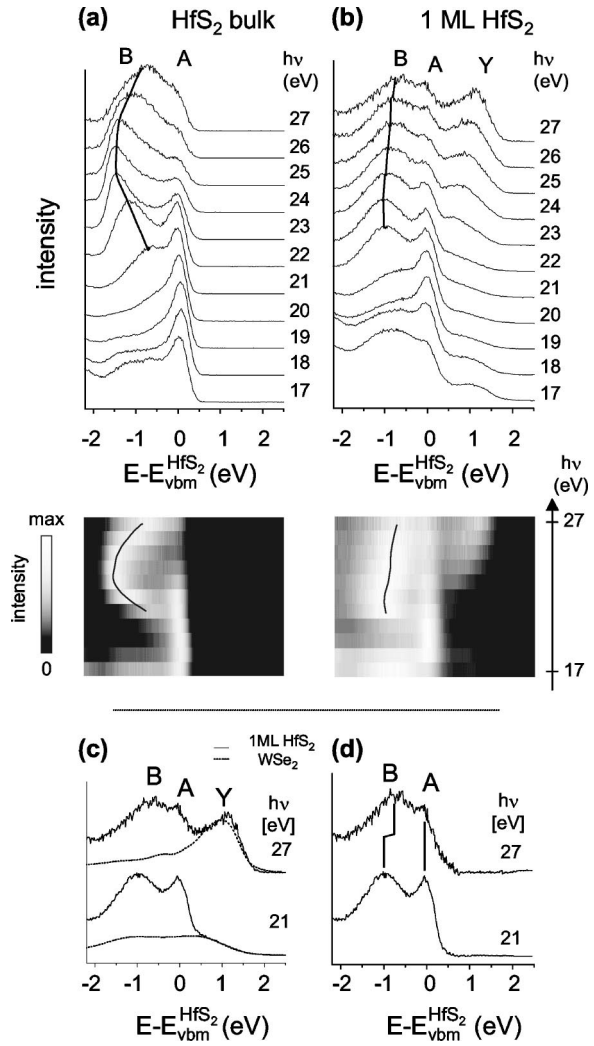

FIG. 2. Angle-resolved photoemission data (normal emission, $k_\parallel=0$) with various photon energies $h\nu$ of (a) HfS_2 bulk crystal and (b) 1 ML HfS_2/WSe_2 (top) and corresponding spectra as gray scale images (bottom). The dispersion of peak *B* is followed by a solid line in the spectra as well as in the gray scale images. (c) Photoemission spectra (normal emission, $k_\parallel=0$) at $h\nu=27$ eV and 21 eV of 1 ML HfS_2/WSe_2 (solid line) and WSe_2 spectra (dotted line) broadened and normalized to match peak *Y* (Ref. 16). (d) Difference between spectra of 1 ML HfS_2/WSe_2 and WSe_2 shown in (c).

slightly changes its binding energy. This difference is easily explained considering a Mulliken analysis of the respective calculated bands. Emission *A* mainly originates from S $3p_x$ and S $3p_y$ derived electronic states which are primarily localized within the layers and interact only very little perpendicular to the layers. In contrast, peak *B* corresponds to electronic states which are derived by more than 90% from S $3p_z$ orbitals. These possess large overlap across the van der Waals gap, leading to the distinct dispersion of band *B* with electron wave vector $k_\perp$.

Angle-resolved photoemission spectra for one monolayer HfS_2 on bulk WSe_2 are shown in Fig. 2(b). Due to the surface sensitivity of photoemission, mainly contributions of the HfS_2 layer are visible in the spectra. Structures *A* and *B* correspond to HfS_2-surface-layer-derived states and may be

compared to structures *A* and *B* of bulk HfS_2. Again, peak *A* does not show any $k_\perp$ dispersion in analogy to the corresponding weakly dispersing structure of the bulk material since the respective states are primarily localized within the HfS_2 monolayer and do not couple to WSe_2 bulk states, therefore. These states are completely localized at the surface and may be regarded as purely two-dimensional surface-layer-derived states.

In contrast, peak *B* which is associated with S $3p_z$ orbitals does show a distinct $k_\perp$ dispersion between photon energies from 21 eV to 27 eV. This becomes also obvious comparing the gray scale images. An additional emission labeled *Y* with increasing intensity at higher photon energies occurs within the band gap of HfS_2. This peak is due to the WSe_2 substrate and does not alter the observed dispersion of peak *B*. To estimate the WSe_2 contributions to the photoelectron current a WSe_2 bulk spectrum is broadened and normalized to match peak *Y* in the spectra at $h\nu = 21$ eV and 27 eV [see Fig. 2(c)]. Subtracting the broadened WSe_2 spectra from the HfS_2 monolayer spectra [see Fig. 2(d)] leaves the dispersion of peak *B* unchanged amounting to ≈ 250 meV [see Fig. 2(d)]. This is a remarkable result in view of the earlier findings by Klein *et al.*[8] who investigated InSe adlayers on graphite. These authors observed that at a thickness of one monolayer of InSe on graphite the InSe valence states do not interact with the substrate at all; i.e., they are electronically fully decoupled and do not show any dispersion, therefore. The dispersion of peak *B* in our current system can only be caused by an interaction between the HfS_2 monolayer and the WSe_2 substrate across the heterointerface. To understand the origin of this unexpected three-dimensional electronic coupling and to identify the WSe_2 band involved in the interaction with the S $3p_z$ orbitals the band lineup between HfS_2 and WSe_2 has to be determined.

The valence band maximum of WSe_2 has been located 0.37 eV above peak *Y* in the spectrum taken at $h\nu = 27$ eV [Fig. 2(c)] applying band mapping and using symmetry properties of the crystal.[15] Since the position of peak *Y* is clearly observable at 1.16 eV above the HfS_2 valence band maximum, we determine the valence band offset $\Delta E_{\mathrm{vbm}} = 1.53 \pm 0.05$ eV.

The WSe_2 band responsible for the coupling can now be identified. To this end, the electronic band structure of WSe_2 is plotted in Fig. 3(a) along the Δ line, which corresponds to the direction perpendicular to the layers in real space [Fig. 3(b)]. Figure 3(c) displays a photoemission spectrum of one monolayer (1 ML) HfS_2 shifted by ΔE_{vbm}. The gray area marks the energy interval over which the emission peak *B* disperses for photon energies between $h\nu = 21$ eV and 27 eV. This energy region coincides with the WSe_2 band *U* which is responsible for the coupling to the electronic HfS_2 monolayer states giving rise to peak *B*.

Figure 3(d) shows the band structure of bulk HfS_2 along the Δ line. Four groups of bands labeled *A*–*D* are associated with the four peaks in the photoelectron spectrum of 1 ML HfS_2 [Fig. 3(c)]. The centers of these bands are marked by circles and clearly coincide with the positions of peaks *A*–*D* in the spectrum of Fig. 3(c). These centers are characteristic

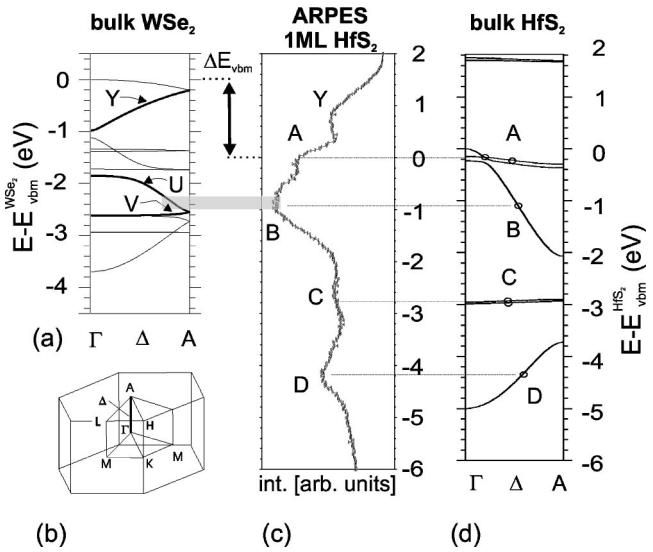

FIG. 3. (a) Electronic band structure of bulk WSe_2 along the Δ line. (b) Brillouin zone of $2H_b$-WSe_2 (c) Photoelectron spectrum of 1 ML HfS_2/WSe_2 (normal emission, $k_\parallel = 0$, $h\nu = 24$ eV) shifted by valence band offset ΔE_{vbm} with respect to the WSe_2 band structure shown in (b). Gray area displays energy interval over which peak *B* disperses with various photon energies. (d) Electronic band structure of bulk HfS_2 along Δ. Centers of the bandwidth are marked by circles.

of a HfS_2 monolayer and the bulk bands develop from them while going from one monolayer to a bulk crystal.

To illustrate the mechanism of three-dimensional coupling between overlayer and substrate the charge densities of electronic states of a HfS_2 monolayer and bulk WSe_2 are exemplarily plotted in Fig. 4. A cut perpendicular to the sandwich layers is shown. The charge densities related to the bands *A*

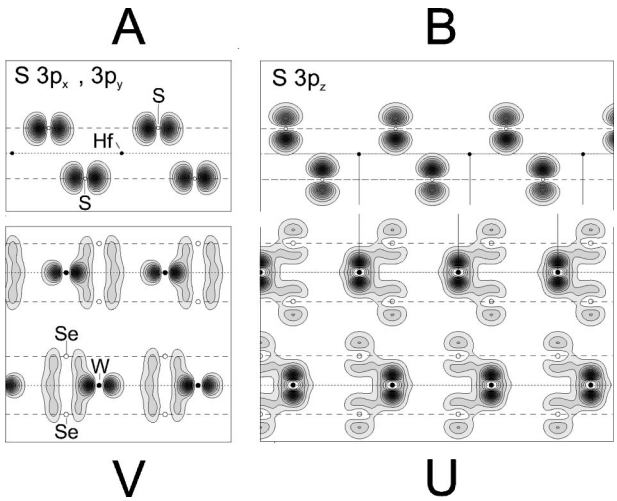

FIG. 4. Charge densities of electronic states of a HfS_2 monolayer at $\frac{1}{2}\Gamma A$ (bands *A* and *B*) and of bulk WSe_2 at $\frac{1}{2}\Gamma A$ (bands *U* and *V*) in the (110) plane. Atomic positions are indicated by solid (Hf and W atoms) and open (S and Se atoms) circles. At the interface between HfS_2 and WSe_2 the positions of Hf and W atoms (see the right panel) are marked by vertical lines. This clearly shows the lateral offsets in the positions of the HfS_2 and WSe_2 atoms.

and V are clearly localized inside the respective layers. The bands U and B, on the other hand, give rise to a high electron density between the HfS_2 monolayer and the WSe_2 substrate. A Mulliken analysis yields a 30% contribution of Se $4p_z$ orbitals to band U and a 90% contribution of S $3p_z$ orbitals to band B at $\frac{1}{2}\Gamma A$. Thus both bands U and B contribute high charge densities across the interface.

This unexpected coupling is even more surprising in view of the fact that there is a substantial lattice mismatch ($\approx 11\%$) between the lattice constants of HfS_2 and WSe_2. In consequence the overlap of the S $3p_z$ and the Se $4p_z$ wave functions is partially reduced at the heterointerface as indicated in Fig. 4. When one Hf atom is located at a matching position (i.e., vertically above a W atom), the neighboring Hf atoms show already considerable lateral shifts with respect to the corresponding W atoms (see the vertical lines in Fig. 4). Accordingly the lower left sulphur orbital (related to band B) can overlap without distortion with the Se substrate orbital (related to band U) while the overlap of the following sulphur orbitals with the selenium substrate orbitals is reduced due to the lateral shifts of the HfS_2 atoms with respect to the WSe_2 atoms. These inequivalent positions of the sulphur orbitals may lead to slightly varying binding energies of the corresponding S $3p_z$ derived surface layer states. Consequently, emission B of the HfS_2 monolayer exhibits a much broader peak width than the respective structure B of bulk HfS_2 [compare Figs. 2(a) and 2(b)].

In conclusion, we have measured angle-resolved photoemission spectra with various photon energies of one HfS_2 monolayer on bulk WSe_2. We have identified two characteristic surface-layer-derived electronic features. One of them is purely two dimensional in nature and clearly localized in the epitaxial overlayer. The second is a surface resonance which is localized to a considerable extent in the epilayer and exhibits very significant three-dimensional coupling to the Se $4p_z$ states of the WSe_2 substrate despite a large lattice mismatch. This interaction can be understood in terms of calculated band structures of HfS_2 and WSe_2 clearly matching dispersive S $3p_z$ and Se $4p_z$ bands when properly aligned to account for the experimentally determined valence band offset.

The authors wish to thank K. Roßnagel for fruitful discussions. This work was supported in part by the BMBF (Project Nos. 05 SE8 FKA and 05 SE8 PMA) and the Deutsche Forschungsgemeinschaft, Forschergruppe DE 412/21-1.

[1] J. Wilson and A. Yoffe, Adv. Phys. **18**, 193 (1969).
[2] A. Koma, K. Sunouchi, and T. Miyajima, Microelectron. Eng. **2**, 129 (1984).
[3] A. Koma, Thin Solid Films **216**, 72 (1992).
[4] W. Jaegermann, A. Klein, and C. Pettenkofer, *Electron Spectroscopies Applied to Low-Dimensional Structures*, Vol. 24 of *Physics and Chemistry of Materials with Low-Dimensional Structures* (Kluwer Academic, Dordrecht, 2000), p. 317.
[5] W. Jaegermann, *Surface Studies of Layered Materials in Relation to Energy Converting Interfaces*, Vol. 14 of *Physics and Chemistry of Materials with Low-Dimensional Structures: Photoelectrochemistry and Photovoltaics of Layered Semiconductors* (Kluwer Academic, Dordrecht, 1992), p. 195.
[6] M.S. Whittingham, Science **192**, 1126 (1976).
[7] G. Prasad and O. Srivastava, J. Phys. D **21**, 1028 (1988).
[8] A. Klein *et al.*, Phys. Rev. Lett. **80**, 361 (1998).
[9] K. Rossnagel, L. Kipp, M. Skibowski, and S. Harm, Nucl. Instrum. Methods Phys. Res. A **467-8**, 1485 (2001).
[10] P. Hohenberg and W. Kohn, Phys. Rev. **136**, B864 (1964).
[11] G.B. Bachelet, D.R. Hamann, and M. Schlüter, Phys. Rev. B **26**, 4199 (1982).
[12] D.M. Ceperley and B.J. Alder, Phys. Rev. Lett. **45**, 566 (1980).
[13] J.P. Perdew and A. Zunger, Phys. Rev. B **23**, 5048 (1981).
[14] R. Manzke and M. Skibowski, in *Electronic Structure of Solids: Photoemission and Related Data*, edited by A. Goldmann and E. Koch, Landolt-Börnstein, New Series, Vol. III/23b (Springer, Berlin, 1994).
[15] M. Traving *et al.*, Phys. Rev. B **55**, 10 392 (1997).
[16] C. Kreis *et al.*, Europhys. Lett. **52**, 189 (2000).